Autistic-Like Traits and Cerebellar Dysfunction in Purkinje Cell PTEN Knock-Out Mice

Title page

Autistic-like traits and cerebellar dysfunction in Purkinje cell *PTEN* knock-out mice

Dario Cupolillo[a,b], Eriola Hoxha[a,b], Alessio Faralli[a,b], Annarita De Luca[a,b], Ferdinando Rossi[a,b]†, Filippo Tempia[a,b] and Daniela Carulli[a,b]

[a] Department of Neuroscience, Neuroscience Institute of Turin (NIT), University of Turin, Regione Gonzole 10, 10043 Orbassano (Turin), Italy

[b] Neuroscience Institute of the Cavalieri-Ottolenghi Foundation (NICO), University of Turin, Regione Gonzole 10, 10043 Orbassano (Turin), Italy

† In memoriam

Short title: Purkinje cell PTEN-KO and autistic-like behavior

Corresponding author
Daniela Carulli
Neuroscience Institute of the Cavalieri-Ottolenghi Foundation (NICO)
University of Turin
Regione Gonzole 10
10043 Orbassano (Turin)
Italy
Phone: +39-011-6706614; Fax: +39-011-6706621
E-mail: daniela.carulli@unito.it

Abstract

Autism spectrum disorders (ASDs) are neurodevelopmental disorders characterized by impaired social interaction, isolated areas of interest and insistence on sameness. Mutations in *Phosphatase and tensin homolog* (*PTEN*) have been reported in individuals with ASDs. Recent evidence highlights a crucial role of the cerebellum in the etiopathogenesis of ASDs. In the present study we analyzed the specific contribution of cerebellar Purkinje cell (PC) PTEN loss to these disorders. Using the Cre-loxP recombination system, we generated conditional knockout mice in which *PTEN* inactivation was induced specifically in PCs. We investigated PC morphology and physiology as well as sociability, repetitive behavior, motor learning and cognitive inflexibility of adult PC *PTEN* mutant mice. Loss of *PTEN* in PCs results in autistic-like traits, including impaired sociability, repetitive behavior and deficits in motor learning. Mutant PCs appear hypertrophic and show structural abnormalities in dendrites and axons, decreased excitability, disrupted parallel fiber and climbing fiber synapses and late-onset cell death. Our results unveil new roles of PTEN in PC function and provide the first evidence of a link between the loss of PTEN in PCs and the genesis of ASD-like traits.

Introduction

Autism spectrum disorders (ASDs) are complex neurodevelopmental disorders affecting around 1% of the population worldwide. ASDs are characterized by abnormal social interaction, deficits in verbal and nonverbal communication, repetitive behaviors and restricted interests (Lai *et al*, 2014). Mutation of *phosphatase and tensin homolog missing on chromosome 10* (*PTEN*) is a causative factor in 5-10% of autism patients (Li *et al*, 1997; McBride *et al*, 2010). PTEN is a lipid and protein phosphatase which dephosphorylates phosphatidylinositol-3,4,5-trisphosphate, negatively regulating the phosphoinositol-3 kinase (PI3K)-AKT-mammalian target of rapamycin (mTOR) signaling pathway, which stimulates protein synthesis and survival, and the AKT/glycogen synthase kinase 3 (GSK3) pathway, which drives cell survival, proliferation and cellular metabolism (Song *et al*, 2012). Mouse models with *PTEN* germline haploinsufficiency show deficits in sociability and increased repetitive behavior, along with brain overgrowth (Clipperton-Allen and Page, 2014, 2015). Conditional knockout mice with *PTEN* deletion in neurons of the cerebral cortex and hippocampus develop macrocephaly due to neuronal hypertrophy and show behavioral abnormalities reminiscent of ASDs (Kwon *et al*, 2006).

Traditionally, the neurological basis of ASD has been thought to lie in the cerebral cortex. However, recent evidence has highlighted a crucial role of the cerebellum in this pathology (Courchesne *et al*, 2001; Fatemi *et al*, 2012; Wang *et al*, 2014). The cerebellum is involved not only in the control of balance, motor coordination and learning, but also in higher order emotional, social and cognitive functions, mainly through its projections (via the thalamus) to various cortical regions including the prefrontal, parietal and limbic cortex (Fatemi *et al*, 2012; Reeber *et al*, 2013; Strick *et al*, 2009). Notably, Purkinje cell (PC) loss is one of the most common anatomical abnormalities seen in autopsy studies of autistic patients (Palmen *et al*, 2004; Whitney *et al*, 2008; Skefos *et al*, 2014; Wegiel *et al*, 2014). Cerebellar injury has been associated with a high incidence of ASDs (Wang *et al*, 2014), and patients with diseases confined to the cerebellum often demonstrate

abnormalities seen in ASDs (Schmahmann, 1998). Recent works have established a strong link between abnormal PC function, caused by the loss of tuberous sclerosis complex (TSC), and behavioral deficits that are relevant to ASDs (Tsai *et al*, 2012; Reith *et al*, 2013). However, to date it is not known whether selective *PTEN* loss-of-function in PCs contributes to the development of ASD traits. To address this issue, we employed conditional knockout mice lacking *PTEN* specifically in PCs. In those mice we observed ASD-like features, including impaired sociability and repetitive behavior, associated with substantial alterations in PC electrophysiological properties and morphological features, ending with PC loss.

Materials and methods

Experimental mice

PTEN conditional knock-out mice (L7/Cre; *PTEN*$^{fl/fl}$, named PTEN-KO) were obtained by crossing L7/Cre transgenic mice, in which Cre expression is driven by the PC-specific promoter L7, with mice bearing LoxP sites flanking *PTEN* exon 5. As ASDs show a higher incidence in males than females (Lai *et al*, 2014), the experiments were conducted on male mice. Further details can be found in Supplementary Materials and Methods.

Genotyping. The presence of Cre and PTEN$^{fl/fl}$ sequences was assessed by PCR. Primer sequences and PCR conditions are reported in **Table S1**.

Histological examination. Methods used for immunostaining and quantification analysis can be found in Supplementary Materials and Methods.

Electrophysiological recordings

Male PTEN-KO and WT mice of 12-18 weeks of age were used. Detailed information can be found in Supplementary Materials and Methods.

Behavioral testing

All behavioral experiments were conducted on male mice of 3-4 months of age (if not specified otherwise) between 9:00 AM and 4:00 PM. Detailed information can be found in Supplementary Materials and Methods.

Statistical analysis

Detailed information can be found in Supplementary Materials and Methods.

Results

PTEN-KO PCs undergo substantial morphological alterations

To evaluate whether the lack of *PTEN* in PCs contribute to the development of ASD-like behavior, we generated conditional knockout mice in which *PTEN* is specifically deleted in PCs (PTEN-KO mice). Although the L7 promoter is also expressed in retinal bipolar neurons (Oberdick *et al*, 1990), the L7/CRE mouse line we used show only a few L7-driven β-galactosidase-positive cells in the latter neurons (Barski *et al*, 2000). Cre expression is evident in PCs by postnatal day 6 and it is fully established by 2-3 weeks after birth (Barski *et al*, 2000). We found that PTEN-KO mice did not show reduced survival or fertility and displayed basic cerebellar architecture. A reliable marker for impaired PTEN function is the upregulation of phosphorylated ribosomal protein S6 (p-S6) (Park *et al*, 2008), a downstream effector of mTOR signaling, which is inhibited by PTEN activity (Song *et al*, 2012). We found increased p-S6 staining in PCs of PTEN-KO mice at 1 month of age (Student's *t*-test $t_{(122)}$=5.22, P<0.001; **Figure 1A-C**), as well as at 4 months of age (**Figure S1**), while no difference between mutants and wild-type (WT) was detected in other brain regions (**Figure S1**).

In all cerebellar lobules PTEN-KO PCs showed enlarged soma. Quantification of the area of PC soma in two different lobules, the IV-V and the IX lobule (**Figure 2F**), showed that PC soma size was increased by 25% in the IV-V lobule (Student's *t*-test $t_{(15)}$=6.57, P<0.001) and 15% in the IX lobule at 2 months of age (Student's *t*-test $t_{(15)}$=4.42, P<0.001), and reached a 50% increase at 4 months (IV-V lobule: Student's *t*-test $t_{(17)}$=16.66, P<0.001; IX lobule: $t_{(17)}$=11.86) and a 60%

increase at 9 months in both lobules (IV-V lobule: Student's *t*-test $t_{(16)}$=16.67, P<0.001; IX lobule: $t_{(14)}$=14.64; **Figure 2A-E', H**, **Figure S2A, B**). Moreover, starting from 2 months of age, PCs of mutant mice showed thicker dendrites and axons when compared to WT PCs, and developed focal dendritic swellings and axonal rounded varicosities (called torpedoes) (**Figure 2A-E'**, **Figure S2A-D**), which became more widespread with age. Namely, the density of dendritic swellings (number/mm^2 area of molecular layer) in the IV-V lobule was 21.13 ± 1.87 at 2 months, 33.24 ± 4.54 at 4 months and 33.94 ± 2.81 at 9 months, and in the IX lobule 48.66 ± 3.96 at 2 months, 58.66 ± 4.54 at 4 months and 118.98 ± 16.34 at 9 months. The density of torpedoes (number/mm^2 area of granule cell layer) in the IV-V lobule was 39.21 ± 5.24 at 2 months, 71.67 ± 4.68 at 4 months and 46.14 ± 3.80 at 9 months, and in the IX lobule 39.06 ± 4.79 at 2 months, 71.78 ± 6.60 at 4 months and 47.83 ± 4.74 at 9 months. Dendritic swellings often displayed abnormal radial outgrowth of dendritic branches (**Figure S2B, C**), and hypertrophic spines were observed on thicker dendrites (**Figure S2E-F'**). Torpedoes, which were mainly located along the axon proximal segment and in many instances were in close proximity to one another in the same axon, displayed a smooth surface, although occasional sprouts could be detected (**Figure S2B, D**). Consistent with PC soma and dendritic enlargement, the thickness of the molecular layer was increased in 2 and 4 months-old PTEN-KO [**Figure 2A-C'**; IV-V lobule: from 151.58 ± 1.64 µm in WT mice to 185.68 ± 2.39 µm in 2 month-old KOs (Dunnett's post hoc $F_{(3,38)}$=193.6, P<0.001), and 173.46 ± 2.33 µm in 4 mo-old KOs (P<0.001); IX lobule: from 141.76 ± 1.28 µm in WT mice to 175.46 ± 1.51 µm in 2 month-old KOs (Dunnett's post hoc $F_{(3,32)}$=134.4, P<0.001), and 171.77 ± 1.14 µm in 4 mo-old KOs (P<0.001)]. Overgrowth of PCs also concerned their axon terminals. PC boutons, which were visualized by double staining for calbindin and VGAT, showed a progressive increase in size with time, which was particularly remarkable after 6 months of age [1.5 fold-increase at 4 months (Student's *t*-test $t_{(396)}$=10.57, P<0.001), 3 fold-increase at 6 months (Student's *t*-test $t_{(241)}$=7.31, P<0.001) and 9 months (Student's *t*-test $t_{(192)}$=6.91, P<0.001); **Figure S3A-F**].

Reduced PC number is one of the most consistent pathological features of ASD patient (Palmen *et al*, 2004; Whitney *et al*, 2008; Skefos *et al*, 2014; Wegiel *et al*, 2014). We found a reduction of PC number in PTEN-KO mice at 6 months of age, when PCs in both IV-V and IX lobule decreased by approximately 50% when compared to WT mice (IV-V lobule: Student's *t*-test $t_{(10)}$=9.42, P<0.001; IX lobule: $t_{(12)}$=14.27, P<0.001) and PTEN-KO mice of younger age (**Figure 2A-E', G**). In 9 month-old PTEN-KO mice, PC number was similar to that of 6 month-old PTEN-KO mice (Student's *t*-test $t_{(16)}$=1.46, P=0.16 and Student's *t*-test $t_{(16)}$=0.52, P=0.61 in IV-V and IX lobule, respectively; **Figure 2D, E', G**), while PCs were further decreased (60%) at 12 months (not shown). In parallel, a reduction in the number of PC axon boutons was found. A 20% decrease was already detected at 4 months of age (Student's *t*-test $t_{(59)}$=4.66, P<0.001; **Figure S3A, C, G**), even without apparent PC loss, suggestive of retraction of the terminal arborization. At later time points, in parallel with massive PC death, considerable decrease in the number of PC axon terminals was evident (70% decrease at 6 and 9 months of age, Student's *t*-test $t_{(38)}$=10.04, P<0.05, Student's *t*-test $t_{(42)}$=18.12, P<0.001, respectively; **Figure S3D, E, G**). Consistent with PC death, the thickness of the mutant molecular layer was decreased from 6 months of age when compared to the thickness of 4 month-old PTEN-KO mice (**Figure 2C-E'**; IV-V lobule: from 173.46 ± 2.33 μm to 115.73 ± 2.13 μm in 9 month-old KOs, P<0.001; IX lobule: from 171.77 ± 1.14 μm to 143.44 ± 2.18 μm in 9 month-old KOs, P<0.001).

To assess whether PC death was due to apoptosis, we analyzed PTEN-KO cerebella from 9 month-old mice for the expression of the apoptosis marker cleaved caspase-3. A few PCs positive for cleaved caspase-3-positive (approximately 1 cell/slice) were detected in mutant animals (**Figure S4A, B**), whilst no cleaved caspase-3-positive PCs were found in WT mice, indicating that apoptosis is one mechanism of PC death in mutant mice.

Abnormal focal swellings of dendritic shafts (accompanied by abnormally high levels of the microtubule-associate protein MAP1B and tubulins), axonal torpedoes and neuronal degeneration

have been observed in PCs of mutant mice lacking MAP1A (Liu *et al*, 2015). The presence of similar dendritic and axonal features in PTEN mutant PCs prompted us to investigate the organization of cytoskeletal components, such as microtubules and neurofilaments. We analyzed MAP2, acetylated α-tubulin and neurofilaments. We found a remarkable increase of neurofilaments content in all PC compartments of PTEN-KO PCs (Student's *t*-test $t_{(115)}$=12.23, P<0.001; **Figure 3A-B', G**), in accordance with previous evidence in the same mouse line (Nayeem *et al*, 2007). MAP2 and acetylated α-tubulin were expressed at higher levels in mutant PC dendrites (MAP2: Student's *t*-test $t_{(48)}$=3.89, P<0.001, acetylated α-tubulin: Student's *t*-test $t_{(66)}$=9.11, P<0.001) and were particularly accumulated in dendritic swellings (**Figure 3C-F', H, I**). Altogether, these data suggest that PTEN is important for the maintenance of microtubule and neurofilament structures that are pivotal for the normal morphology of PCs.

Deficits of spontaneous and evoked firing activity of PTEN-KO PCs

By means of cell-attached patch-clamp recordings we measured the action potential firing of single PCs during block of the main excitatory and inhibitory ionotropic receptors. In the spontaneous firing activity, the mean interspike interval (ISI) in PTEN-KO PCs was significantly increased with respect to WT mice [(KO cells (n = 18): 65.61 ± 8.01 ms; WT cells (n = 19): 37.85 ± 4.38 ms, Student's t-test $t_{(35)}$=3.08, P<0.05] without significant changes in the regularity of firing (coefficient of variation, KO: 0.13 ± 0.03; WT: 0.09 ± 0.03; Student's *t*-test $t_{(34)}$=1.16, P>0.05) (**Figure 4A-D** and **Table S2**). In order to study the mechanisms responsible for the reduced spontaneous firing, we studied evoked action potentials. In response to hyperpolarizing stimuli, PTEN-KO PCs showed a lower input resistance (-54.5 ± 6.5 MΩ, n = 13) relative to WT neurons (-70.9 ± 4.0 MΩ, n = 12; Student's *t*-test $t_{(29)}$=2.18, P<0.05) (**Figure 4E, F**). On the contrary, no significant changes were observed for the bump due to the I_H current (Student's *t*-test $t_{(29)}$=1.15, P>0.05; **Figure 4G** and **Table S2**). In line with the reduction of spontaneous firing, also in the evoked discharge PTEN-KO PCs fired action potentials with a lower frequency at all stimulus intensities (**Figure 4H, I**). In

accordance with this result, PTEN-KO PCs displayed a more pronounced frequency adaptation with significantly prolonged 2nd, 3rd and 10th ISI (Student's *t*-test, $t_{(13)}$=2.78, P<0.05; $t_{(12)}$=3.58, P<0.01, and $t_{(12)}$=3.46, P<0.01, respectively) (**Figure 4J, K** and **Table S2**). The latency of the first spike was highly variable and displayed a tendency to longer values (**Table S2**). The other parameters of action potential were comparable between PTEN-KO and WT PCs (**Table S2**). These data, taken together, corroborate the finding of a reduced excitability of PTEN-KO PCs.

Altered excitatory postsynaptic currents in PTEN-KO PCs

Parallel fibers (PF) were stimulated with intensities ranging from 3 to 15 μA. The PF-EPSC amplitudes in PTEN-KO mice were significantly higher than in WT from stimulus intensity 6 to 15 μA (WT: n = 20; KO: n = 20; two-way repeated measures ANOVA $F_{(1,152)}$=6.15, P<0.05); **Figure 4L, M**). This result indicates that the basal synaptic transmission is altered. To better understand if the changes in this synapse are pre- or post-synaptic we performed paired-pulse stimulation with variable inter-stimulus interval. The time course of paired-pulse facilitation was similar in WT and PTEN-KO PCs at all inter-stimulus intervals (from 50 to 200 ms; two-way repeated measures ANOVA $F_{(1,34)}$=0.38, P>0.05; **Figure 4N**). The equal values of paired pulse facilitation across the genotypes indicate that the changes in PF-PC synapse are postsynaptic, in accordance with the severe dysmorphisms of PC dendrites.

The balance between PF and climbing fiber (CF) inputs is disrupted in other murine models of autism (Baudouin *et al*, 2012). Therefore, we decided to investigate the other excitatory input to PCs, the CF synapse. The amplitude of CF-EPSCs was reduced in PTEN-KO PCs (**Figure 4O, P**; KO: 0.41 ± 0.12 nA, n = 11; WT: 0.77 ± 0.12 nA, n = 9; Mann Whitney test P<0.05). To test whether such a decreased synaptic size of the CF-PC synapse was due to pre- versus post-synaptic mechanisms, we analyzed its short-term depression, which is known to be affected selectively by presynaptic changes (Hashimoto and Kano, 1998). At short and intermediate inter-stimulus intervals, between 50 and 400 ms, PTEN-KO PCs displayed a reduced short-term depression

relative to WT (**Figure 4Q**; two-way repeated measures ANOVA $F_{(1,16)}$=8.99, P<0.01). The time course of short-term depression was described by double exponential functions with the following fast and slow time constants and relative amplitudes: WT, τ_f = 208.2 ms, 46.7%; τ_s = 2.93 s, 53.3%; KO, τ_f = 260.2 ms, 61.4.%; τ_s = 11.31 s, 38.6%. These results on the CF synapse are consistent with a presynaptic deficiency.

PTEN-KO mice show repetitive behavior

All behavioral tests were performed before the onset of PC death, namely at 3-4 months of age. Among stereotyped/repetitive behaviors, we analyzed grooming and upright scrabbling/jumping. Upright scrabbling consists in a fast, rhythmic movement of the forepaws, and sometimes of one hind paw as well, against the cage walls while the mouse is standing in an upright position (**Video S1**). This behavior, which sometimes was mixed with jumping, has been previously observed in ASD-mouse models (Ryan *et al*, 2010; Muehlmann and Lewis, 2012; Won *et al*, 2012). In PTEN KO mice, grooming was decreased (88.56 ± 16.83 sec in WT vs 35.00 ± 11.62 sec in KOs, Student's *t*-test $t_{(19)}$=2.69, P<0.05; **Figure 5B**), while upright scrabbling/jumping was greatly enhanced (7.50 ± 3.67 sec in WT vs 129.09 ± 20.15 sec in KOs, Student's *t*-test $t_{(19)}$=5.66, P<0.001; **Figure 5A**). This behavior was present in all analyzed PTEN-KO mice (in which it lasted more than 60 sec), while shorter bouts of this behavior were only seen in 2 out of 10 WT mice (lasting 21 and 35 sec, respectively; **Figure S5**).

PTEN-KO mice show abnormal social behavior

In the three-chambered assay of sociability, WT mice spent significantly more time in the chamber with the stranger mouse than in the chamber with the object (284.66 ± 15.32 sec vs 154.60 ± 9.11 sec, Student's paired *t*-test $t_{(19)}$=6.22, P<0.001; **Figure 5C**). In contrast, PTEN-KO mice showed no preference for the stranger mouse (260.30 ± 14.64 sec vs 236.00 ± 11.79 sec, Student's paired *t*-test $t_{(23)}$=1.06, P=0.30; **Figure 5C**). The social behavior was further tested by assessing the social interaction with a female conspecific. We observed a significant reduction in the time spent by male

PTEN-KO mice sniffing, allogrooming, mounting or following the female with respect to WT (59.70 ± 12.13 out of 180 sec, i.e. 33% of the time in KO vs 111.30 ± 8.24 sec, i.e. 62% in WT mice; Student's *t*-test $t_{(18)}$=3.52, P<0.01; **Figure 5D**). To exclude that the impaired sociability score was due to locomotor deficits or bouts of repetitive behavior, we measured the distance travelled by the mice during the social approach test and in the open field. In the three-chamber apparatus, in both the habituation and test phase, locomotion was not significantly different between genotypes (distance travelled in the habituation phase, WT: 4318 ± 283 cm; KOs: 4391 ± 218 cm, Student's *t*-test $t_{(42)}$=0.20, P=0.84; in presence of stimuli, WT: 3358 ± 222 cm, KO: 3463 ± 120 cm; Student's *t*-test $t_{(42)}$=0.43, P=0.68). Also in the open field, the distance travelled by the mice was comparable in WT and mutants (WT: 3827.73 ± 213.11 cm, KO: 4153.58 ± 327.62 cm; Student's *t*-test $t_{(19)}$=0.85, P=0.41).

Spatial learning and cognitive flexibility are preserved in PTEN-KO

To model cognitive inflexibility, which may be exhibited by patients with ASDs, we tested animals in a reversal learning paradigm using a Morris water maze or a water T-maze. In both the acquisition phase and the probe trial of Morris water maze, WT and PTEN-KO mice showed similar results (acquisition phase: two-way repeated measures ANOVA $F_{(1,23)}$=0.24, P>0.05; probe trial: Student's *t*-test for target area $t_{(23)}$=0.53, P=0.60; **Figure S6A, B**). In the reversal phase, the latency to find the platform of PTEN-KO mice was comparable to that of WT mice over 2 days of training (two-way repeated measures ANOVA $F_{(1,23)}$=1.94, P>0.05; **Figure S6C**), and the percentage of time spent in the target zone in the probe trial was similar to that of WT (Student's *t*-test $t_{(23)}$=0.05, P=0.96; **Figure S6D**). We also tested PTEN-KO mice in the reversal water T-maze test. On the 1st acquisition day, mutant animals had similar acquisition learning compared to WT mice (number of correct trials: Student's *t*-test $t_{(18)}$=1.34, P=0.20; number of trials prior to 5 consecutive correct trials: Student's *t*-test $t_{(18)}$=1.02, P=0.32; **Figure S6E, F**). In the reversal phase, mutant mice did not show any impairment in learning of the new platform location (I day, number of correct trials:

Student's *t*-test $t_{(17)}$=0.93, P=0.37; number of trials prior to 5 consecutive correct trials: Student's *t*-test $t_{(17)}$=0.19, P=0.85; II day: number of correct trials: Student's *t*-test $t_{(17)}$=0.46, P=0.65; number of trials prior to 5 consecutive correct trials: Student's *t*-test $t_{(17)}$=0.15, P=0.88; **Figure S6E, F**).

Coordination and motor learning in PTEN-KO mice

Since patients with ASDs can show anomalous motor learning associated with cerebellar defects (Marko *et al*, 2015), we investigated whether PTEN-KO mice showed motor deficits in the rotarod test. In 2-3 months-old mice, the latency to fall was not significantly different between genotypes (two-way repeated measures ANOVA $F_{(1,13)}$=1.28, P>0.05; **Figure S7A**). However, at 5-6 months of age, PTEN-KO mice tended to have a shorter latency than WT mice on the 1st day (two-way repeated measures ANOVA $F_{(1,11)}$=12.94, Bonferroni post hoc P=0.09) and showed no improvement with time (**Figure S7B**; WT vs KOs: Bonferroni post hoc P<0.01 on 2nd day, P<0.01 on 3rd day), indicating deficits in motor coordination and learning in association with ongoing PC loss.

Discussion

In this study we provide evidence that PTEN in cerebellar PCs plays a key role in mechanisms involved in ASDs. We show that mice with a selective disruption of PTEN in PCs display behavioral traits related to ASDs, associated with abnormal signaling and aberrant morphology of PCs.

Behavioral features

The three core symptoms of ASD are impairment in social interaction, communication, and the propensity for restricted, repetitive behaviors (Lai *et al*, 2014). Several mouse models of ASD are currently available, which reproduce one or more of these core symptoms (Pasciuto *et al*, 2015). PTEN-KO mice displayed a severe impairment in social interaction. Moreover, a repetitive behavior was present, namely upright scrambling/jumping, in line with the finding of a single type

of repetitive behavior in each ASD-mouse model (Ryan *et al*, 2010; Muehlmann and Lewis, 2012; Won *et al*, 2012).. Self-grooming was decreased, likely because of the longer time spent in the stereotyped behavior of jumping/scrabbling reduced the time left for physiological grooming. Taken together, the deficits in sociability and the presence of a restricted repetitive behavior validate PTEN-KO mice as a model of ASDs. In order to distinguish ASD-related symptoms from mental retardation, it is necessary to exclude cognitive impairment. Indeed, PTEN-KO mice showed a normal performance in all cognitive tests, including cognitive flexibility.

In addition to the symptoms directly related to ASD, PTEN-KO mice also displayed impaired motor learning in the rotarod test in concomitance with PC loss. This motor deficit was expected, since motor performance requires a proper function of the cerebellar network. Indeed, it has also been observed in a number of other mutants displaying PC loss (see for review Porras-Garcia et al, 2013). Nonetheless, gait abnormalities or other types of motor symptoms are often present in ASD patients as well, and they have been related to cerebellar malformation (Marko *et al*, 2015).

PC functional alterations

Alterations in the generation of PC action potentials have been classically considered responsible for cerebellar motor deficits and, more recently, for ASD-related symptoms (Tsai *et al*, 2012). In our study we found that PTEN-KO PCs have a lower frequency of spontaneous firing, are less excitable and have a smaller input resistance. The reduction in input resistance can be responsible, at least in part, for the lower excitability. A reduced firing frequency and input resistance were previously described also in PC-selective *Tsc1* knock-out mice (Tsai *et al*, 2012), which also display an autistic-like behavior, suggesting that these features could be common alterations related to this disorder.

The output signals from PCs are finely regulated by impinging synaptic inputs. An increase in excitatory transmission in PTEN-KO models is well documented in several studies in different types of neuronal cells (Luikart *et al*, 2011; Takeuchi *et al*, 2013). Here we report for the first time

in PTEN-KO PCs an increased amplitude of EPSCs evoked by stimulation of the PF-PC synapse. This change seems to be postsynaptic because the paired pulse facilitation is unchanged. On the contrary, the amplitude of EPSCs evoked by stimulation of the CF-PC synapse was reduced and the paired-pulse depression was enhanced in PTEN-KO mice, suggesting a presynaptic mechanism (Hashimoto and Kano, 1998). At this synapse, presynaptic changes induced by postsynaptic signals have been described both during development (Bosman and Konnerth, 2009) and in the adult (Safo *et al*, 2006). Since CFs exert a powerful tonic inhibition on PCs (Montarolo *et al*, 1982), a weaker CF input and a stronger PF synapse have additive effects, resulting in a greatly enhanced excitatory drive. It is interesting to note that in a different model of autism, the neuroligin3 KO mouse, PF- and CF-PC synapses are altered, but in the opposite direction than in PTEN-KO PCs (Baudouin *et al*, 2012). This suggests that an incorrect balance between PF and CF synapses might underlie autistic-like deficiencies.

PC morphological alterations

In this study we show that PTEN plays a key role also in the regulation of PC morphology. The lack of *PTEN* in PCs induced remarkable structural changes, including overgrowth of all PC compartments, axonal and dendritic swellings, abnormal dendritic branching, accumulation of cytoskeletal components and late-onset PC loss. Those findings add to preceding reports of hypertrophy and anomalous morphology in *PTEN*-deleted neurons. Conditional knockout of *PTEN* in post-mitotic neurons of the cerebral cortex and hippocampus induced overgrowth of soma, dendrites and axons, ectopic neuronal processes and increased spine number (Kwon *et al*, 2006). Similarly, *PTEN* silencing promoted the growth and branching of dendrites in cultured hippocampal neurons (Jaworski *et al*, 2005). Notably, hypertrophy was also observed in mice lacking TSC1 or TSC2 in PCs (Tsai *et al*, 2012; Reith *et al*, 2011), which are downstream targets of the PTEN/PI3K pathway. Intriguingly, in our model PTEN appears to have a critical role in modulating the organization/distribution of microtubule networks in the PC dendritic compartment, which are

pivotal for the normal dendritic morphology, intracellular transport and neuronal survival (Liu *et al*, 2015).

PCs and autism

PC loss has been observed in several autopsy studies of autistic patients (Palmen *et al*, 2004; Whitney *et al*, 2008; Skefos *et al*, 2014; Wegiel *et al*, 2014). Regarding animal models, Lurcher chimeric mice, which show cerebellar abnormalities including postnatal loss of PCs, display behavioral inflexibility and repetitive behavior (Martin *et al*, 2010). PC-selective p75 neurotrophin receptor KO mice exhibit less allogrooming and socialization/fighting, and more stereotyped jumping behavior (Lotta *et al*, 2014). Similar features were also strongly evident in our mutants, reinforcing the idea that PCs play a role in the regulation of specific autistic-like traits. In addition, in PC *Tsc1* mutant mice, social and cognitive deficits are associated with increased PC size, altered electrophysiological properties and PC loss (Tsai *et al*, 2012), which remind some of the features observed in our model. As shown by p-S6 increase, TSC/mTOR signaling pathway is one of the downstream pathways mediating the effects of PTEN loss in our model, which may trigger cellular and behavioral alterations such as those observed in PC *Tsc1* and *Tsc2* mutant mice. However, several differences occur between *Tsc1*/*Tsc2* and PTEN-KO mice (Tsai *et al*, 2012; Reith *et al*, 2011), suggesting that PTEN, besides acting on TSC, may also operate through alternative mechanisms, such as AKT/GSK-3 pathway (see Nayeem *et al*, 2007; Marino *et al*, 2002), to induce specific morphological features and behavioral traits. Nonetheless, since deficits in inflexibility are apparent in PC *Tsc1* mutant mice only in concomitance with PC degeneration, but not with PC dysfunction (Tsai *et al*, 2012), we cannot exclude that similar features occur in our model at later stages, when PC loss occurs.

How the cerebellum modulates the abnormal behaviors of autism remains a topic of intense investigation. Autism has been proposed to be a disorder of multiple brain networks, including neocortical substrates (Muller, 2007). The cerebellum is connected, through the cerebellar nuclei, to

these networks, and has been proposed to regulate them. For example, cerebellar output through the cerebellar nuclei modulates dopamine release in the medial prefrontal cortex via dopaminergic projections from the ventral tegmental area and glutamatergic projections from the mediodorsal and ventrolateral thalamus (Mittleman *et al*, 2008; Rogers *et al*, 2011). By affecting cerebellar nuclei activity, PTEN-KO PC dysfunction may thus alter downstream neuronal networks, thereby contributing to autistic-like behaviors.

On the whole, PTEN-KO mice represent a valuable experimental model to investigate the effects of PC dysfunction on ASD-related neuronal networks and to gain a deeper insight on cerebellum-related mechanisms contributing to the pathogenesis of ASDs caused by *PTEN* mutation.

Funding and disclosure

This work was supported by EU Seventh Framework Program (FP7) Marie Curie Actions (AxRegen), MIUR (Ministero dell'Istruzione, dell'Università e della Ricerca) PRIN 20107MSMA4, PRIN 20108WT59Y and ex-60% grants. The authors declare no conflict of interest.

Acknowledgments

We wish to thank Marco Sassoè-Pognetto (University of Turin) for the kind gift of L7/CRE transgenic mice, Angela Longo (University of Turin) for her help with behavioral tests and Annalisa Buffo (University of Turin) for helpful discussion and support.

Supplementary information is available at the *Neuropsychopharmacology* website.

References

Barski JJ, Dethleffsen K, Meyer M (2000). Cre recombinase expression in cerebellar Purkinje cells. *Genesis* **28:** 93-98.

Baudouin SJ *et al*. (2012). Shared synaptic pathophysiology in syndromic and nonsyndromic rodent models of autism. *Science* **338:** 128-132.

Bosman LW, Konnerth A (2009). Activity-dependent plasticity of developing climbing fiber-Purkinje cell synapses. *Neuroscience* **162:** 612-623.

Clipperton-Allen AE, Page DT (2014). Pten haploinsufficient mice show broad brain overgrowth but selective impairments in autism-relevant behavioral tests. *Hum Mol Genet* **23:** 3490-3505.

Clipperton-Allen AE, Page DT (2015). Decreased aggression and increased repetitive behavior in Pten haploinsufficient mice. *Genes Brain Behav* **14:** 145-157.

Courchesne E *et al*. (2001). Unusual brain growth patterns in early life in patients with autistic disorder: an MRI study. *Neurology* **57:** 245-254.

Fatemi SH *et al*. (2012). Consensus paper: pathological role of the cerebellum in autism. *Cerebellum* **11:** 777-807.

Hashimoto K, Kano M (1998). Presynaptic origin of paired-pulse depression at climbing fibre-Purkinje cell synapses in the rat cerebellum. *J Physiol* **506:** 391-405.

Jaworski J, Spangler S, Seeburg DP, Hoogenraad CC, Sheng M (2005). Control of dendritic arborization by the phosphoinositide-3'-kinase-Akt-mammalian target of rapamycin pathway. *J Neurosci* **25:** 11300-11312.

Kwon CH *et al*. (2006). Pten regulates neuronal arborization and social interaction in mice. *Neuron* **50:** 377-388.

Lai MC, Lombardo MV, Baron-Cohen S (2014). Autism. *Lancet* **383:** 896-910.

Li J *et al*. (1997). PTEN, a putative protein tyrosine phosphatase gene mutated in human brain, breast, and prostate cancer. *Science* **275:** 1943-1947.

Liu Y, Lee JW, Ackerman SL (2015). Mutations in the Microtubule-Associated Protein 1A (Map1a) Gene Cause Purkinje Cell Degeneration. *J Neurosci* **35:** 4587-4598.

Lotta LT, Conrad K, Cory-Slechta D, Schor NF (2014). Cerebellar Purkinje cell p75 neurotrophin receptor and autistic behavior. *Transl Psychiatry* **4:** e416.

Luikart BW *et al*. (2011). Pten knockdown in vivo increases excitatory drive onto dentate granule cells. *J Neurosci* **31:** 4345-4354.

Marino S *et al*. (2002). PTEN is essential for cell migration but not for fate determination and tumourigenesis in the cerebellum. *Development* **129:** 3513-3522.

Marko MK *et al*. (2015). Behavioural and neural basis of anomalous motor learning in children with autism. *Brain* **138:** 784-797.

Martin LA, Goldowitz D, Mittleman G (2010). Repetitive behavior and increased activity in mice with Purkinje cell loss: a model for understanding the role of cerebellar pathology in autism. *Eur J Neurosci* **31:** 544-555.

McBride KL *et al*. (2010). Confirmation study of PTEN mutations among individuals with autism or developmental delays/mental retardation and macrocephaly. *Autism Res* **3:** 137-141.

Mittleman G, Goldowitz D, Heck DH, Blaha CD (2008). Cerebellar modulation of frontal cortex dopamine efflux in mice: relevance to autism and schizophrenia. *Synapse* **62:** 544-550.

Montarolo PG, Palestini M, Strata P (1982). The inhibitory effect of the olivocerebellar input on the cerebellar Purkinje cells in the rat. *J Physiol* **332:** 187-202.

Muehlmann AM, Lewis MH (2012). Abnormal repetitive behaviours: shared phenomenology and pathophysiology. *J Intellect Disabil Res* **56:** 427-440.

Muller RA (2007). The study of autism as a distributed disorder. *Ment Retard Dev Disabil Res Rev* **13:** 85-95.

Nayeem N *et al*. (2007). Hyperphosphorylation of tau and neurofilaments and activation of CDK5 and ERK1/2 in PTEN-deficient cerebella. *Mol Cell Neurosci* **34:** 400-408.

Oberdick J, Smeyne RJ, Mann JR, Zackson S, Morgan JI (1990). A promoter that drives transgene expression in cerebellar Purkinje and retinal bipolar neurons. *Science* **248:** 223-226.

Palmen SJ, van Engeland H, Hof PR, Schmitz C (2004). Neuropathological findings in autism. *Brain* **127:** 2572-2583.

Park KK *et al*. (2008). Promoting axon regeneration in the adult CNS by modulation of the PTEN/mTOR pathway. *Science* **322:** 963-966.

Pasciuto E, Borrie SC, Kanellopoulos AK, Santos AR, Cappuyns E, D'Andrea L, Pacini L, Bagni C (2015). Autism Spectrum Disorders: Translating human deficits into mouse behavior. *Neurobiol Learn Mem* **124:** 71-87.

Porras-García ME, Ruiz R, Pérez-Villegas EM, Armengol JÁ (2013). Motor learning of mice lacking cerebellar Purkinje cells. *Front Neuroanat* **7:**4. doi: 10.3389/fnana.2013.00004.

Reeber SL, Otis TS, Sillitoe RV (2013). New roles for the cerebellum in health and disease. *Front Syst Neurosci* **7:** 83.

Reith RM *et al*. (2013). Loss of Tsc2 in Purkinje cells is associated with autistic-like behavior in a mouse model of tuberous sclerosis complex. *Neurobiol Dis* **51:** 93-103.

Reith RM, Way S, McKenna J, 3rd, Haines K, Gambello MJ (2011). Loss of the tuberous sclerosis complex protein tuberin causes Purkinje cell degeneration. *Neurobiol Dis* **43:** 113-122.

Rogers TD *et al*. (2011). Connecting the dots of the cerebro-cerebellar role in cognitive function: neuronal pathways for cerebellar modulation of dopamine release in the prefrontal cortex. *Synapse* **65:** 1204-1212.

Ryan BC, Young NB, Crawley JN, Bodfish JW, Moy SS (2010). Social deficits, stereotypy and early emergence of repetitive behavior in the C58/J inbred mouse strain. *Behav Brain Res* **208:** 178-188.

Safo PK, Cravatt BF, Regehr WG (2006). Retrograde endocannabinoid signaling in the cerebellar cortex. *Cerebellum* **5:** 134-145.

Schmahmann JD (1998). Dysmetria of thought: clinical consequences of cerebellar dysfunction on cognition and affect. *Trends Cogn Sci* **2:** 362-371.

Skefos J *et al.* (2014) Regional alterations in purkinje cell density in patients with autism. *PLoS One* **9:** e81255. doi: 10.1371/journal.pone.0081255.

Song MS, Salmena L, Pandolfi PP (2012). The functions and regulation of the PTEN tumour suppressor. *Nat Rev Mol Cell Biol* **13:** 283-296.

Strick PL, Dum RP, Fiez JA (2009). Cerebellum and nonmotor function. *Annu Rev Neurosci* **32:** 413-434.

Takeuchi K *et al*. (2013). Dysregulation of synaptic plasticity precedes appearance of morphological defects in a Pten conditional knockout mouse model of autism. *Proc Natl Acad Sci U S A* **110:** 4738-4743.

Tsai PT *et al*. (2012). Autistic-like behaviour and cerebellar dysfunction in Purkinje cell Tsc1 mutant mice. *Nature* **488:** 647-651.

Wang SS, Kloth AD, Badura A (2014). The cerebellum, sensitive periods, and autism. *Neuron* **83:** 518-532.

Wegiel J *et al.* (2014). Stereological study of the neuronal number and volume of 38 brain subdivisions of subjects diagnosed with autism reveals significant alterations restricted to the striatum, amygdala and cerebellum. *Acta Neuropathol Commun* **2:** 141.

Whitney ER, Kemper TL, Bauman ML, Rosene DL, Blatt GJ (2008). Cerebellar Purkinje cells are reduced in a subpopulation of autistic brains: a stereological experiment using calbindin-D28k. *Cerebellum* **7:** 406-416.

Won H *et al*. (2012). Autistic-like social behaviour in Shank2-mutant mice improved by restoring NMDA receptor function. *Nature* **486:** 261-265.

Figure legends

Fig. 1. Expression levels of p-S6 are increased in PCs of PTEN-KO mice. PTEN KO mice of 1 month of age demonstrate increased p-S6 staining in PCs (B) when compared to WT mice (A), consistent with increased mTOR signaling from *PTEN* deletion. In (A') and (B'), PCs are stained by anti-calbindin antibodies. In (C) quantification of p-S6 staining intensity in WT and KO PC soma (WT: 45 PCs from 3 animals; KO: 77 PCs from 5 animals). Data shown are means ± SEM. Scale bar: 50 μm in A (also applies to A'-B'). *** P<0.001, Student's unpaired *t* test.

Fig. 2. PTEN-KO mice display abnormal PC morphology and reduced PC number. (A-E') Representative pictures from a 2 month-old WT mouse and KO mice of various ages show calbindin-stained PCs. Mutant PCs, starting from 1 month of age, are hypertrophic. PC dendrites display several enlargements (arrowheads in B'-E'). Numerous swellings are evident along the proximal segment of PC axons (arrows in B'-E'). The thickness of the molecular layer (ML) was increased in KO cerebella at 2 and 4 months of age, while it decreased afterwards. PC loss was apparent in 6 and 9 month-old KO animals (D-E'). (G) shows the quantification of PC density (3 slices/animal from at least 3 animals/each time point), performed in the IV-V and IX lobule (F). (H) shows the quantification of PC soma area (3 slices/animal from at least 3 animals/each time point). Data shown are means ± SEM. Scale bars: 200 μm in A-E, 50 μm in A'-E'. * P<0.05, *** P<0.001, Student's unpaired *t* test.

Fig. 3. Increased levels of cytoskeletal elements in PTEN-KO PCs. In (A-B'), PCs of KO mice display stronger SMI32 staining than WT PCs, including in dendritic enlargements (compare B' with A'). (C') and (D') are representative pictures of WT and KO cerebellum labeled with anti-MAP2 antibodies, which reveal high staining intensity in KO PC dendrites, particularly in their

enlargements. In (E') and (F'), increased levels of acetylated alfa-tubulin are apparent in dendrites of KO PCs when compared to WT ones. (A), (B), (C), (D), (E) and (F) show anti-calbindin staining. (G, H, I) show the quantification of SMI32, MAP2 and ace-tubulin staining intensity, respectively (arbitrary units on the *y* axis). Scale bar: 50 μm in A (also applies to A'-H'). *** P<0.001, Student's unpaired *t* test.

Fig. 4. PC spontaneous and evoked firing activity, PF-EPSCs and CF-EPSCs in PTEN-KO and WT PCs. (A) Representative traces of spontaneous firing in cell attached configuration in a WT (upper trace) and a KO PC (lower trace). (B) Distribution histograms of interspike intervals from the WT and KO PCs shown in A. (C) Mean interspike interval (ISI) of WT (n = 19) and KO (n = 18) PCs. (D) Coefficient of variation (CV) of interspike intervals in WT and KO PCs. (E) Hyperpolarizations evoked by negative current injection (-400 pA) in WT (black) and KO (grey) PCs. (F) Mean input resistance of WT and KO PCs. (G) Mean amplitude of the bump due to the inward rectifier current. (H) Representative traces of firing evoked by injection of depolarizing current. (I) Evoked firing frequency as a function of stimulation intensity. Dashed lines are linear fittings of points above threshold. (J) Representative traces of evoked firing showing the first spikes where the interspike intervals was measured. (K) Mean values of first, second, third and tenth interspike intervals. (L) Representative traces of PF-EPSCs recorded from WT and KO PCs. (M) Input-output curve of PF-EPSCs of WT (n=20) and KO (n=20) mice. (N) PF-EPSC short-term facilitation. The amplitude of the second response is expressed as a percentage of the first response (mean ± SEM) and is plotted as a function of interstimulus intervals. (O) Representative traces of CF-EPSCs recorded from WT and KO PCs. (P) Mean CF-EPSC amplitude in WT (n = 11) and KO (n = 9) mice. (Q) Time course of paired-pulse depression of CF-EPSC in WT (black circles) and KO mice (grey squares). The amplitude of the second response is expressed as a percentage of the first response (mean ± SEM) and is plotted as a function of interstimulus intervals. The dashed lines

are double exponentials fittings of WT and KO data points. Stimulus artifacts have been omitted for clarity. In all panels, WT data are shown in black and KO ones in grey. * P<0.05, ** P<0.01, Student's unpaired *t*-test in (C), (F), (K), (P), two way-ANOVA followed by Bonferroni's *post hoc* analysis in (I), (E), (M), (Q).

Fig. 5. Repetitive behavior and impaired sociability in PTEN-KO mice. PTEN KO mice spend more time doing upright scrabbling mixed with jumping than WT mice (A) and less time self-grooming (B) (WT: n = 10; KOs: n = 11). In the social approach test, WT mice spend more time in the chamber with the stranger animal than in the chamber with the inanimate object, while KO mice show no preference (WT: n = 20; KOs: n = 24; C). Reduced sociability of KO mice is also evident when measuring the time spent interacting with a female conspecific, which is significantly less than that of WT mice (WT: n = 10; KO: n= 10; D). Data shown are means ± SEM. * P<0.05, ** P<0.01, *** P<0.001, Student's unpaired *t*-test in (A), (B) and (D), Student's paired *t*-test in (C).

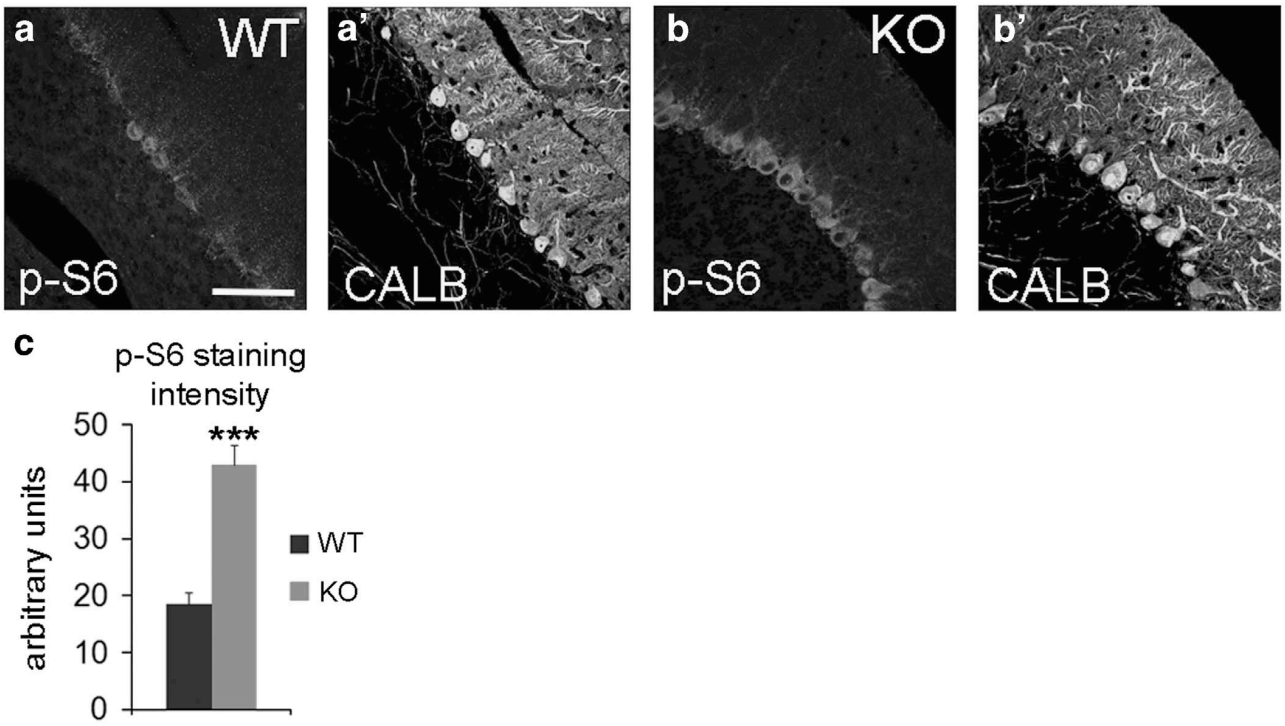
a
WT
p-S6
a'
CALB
b
KO
p-S6
b'
CALB
c
p-S6 staining intensity
***
arbitrary units
50
40
30
20
10
0
WT
KO

Fig. 1

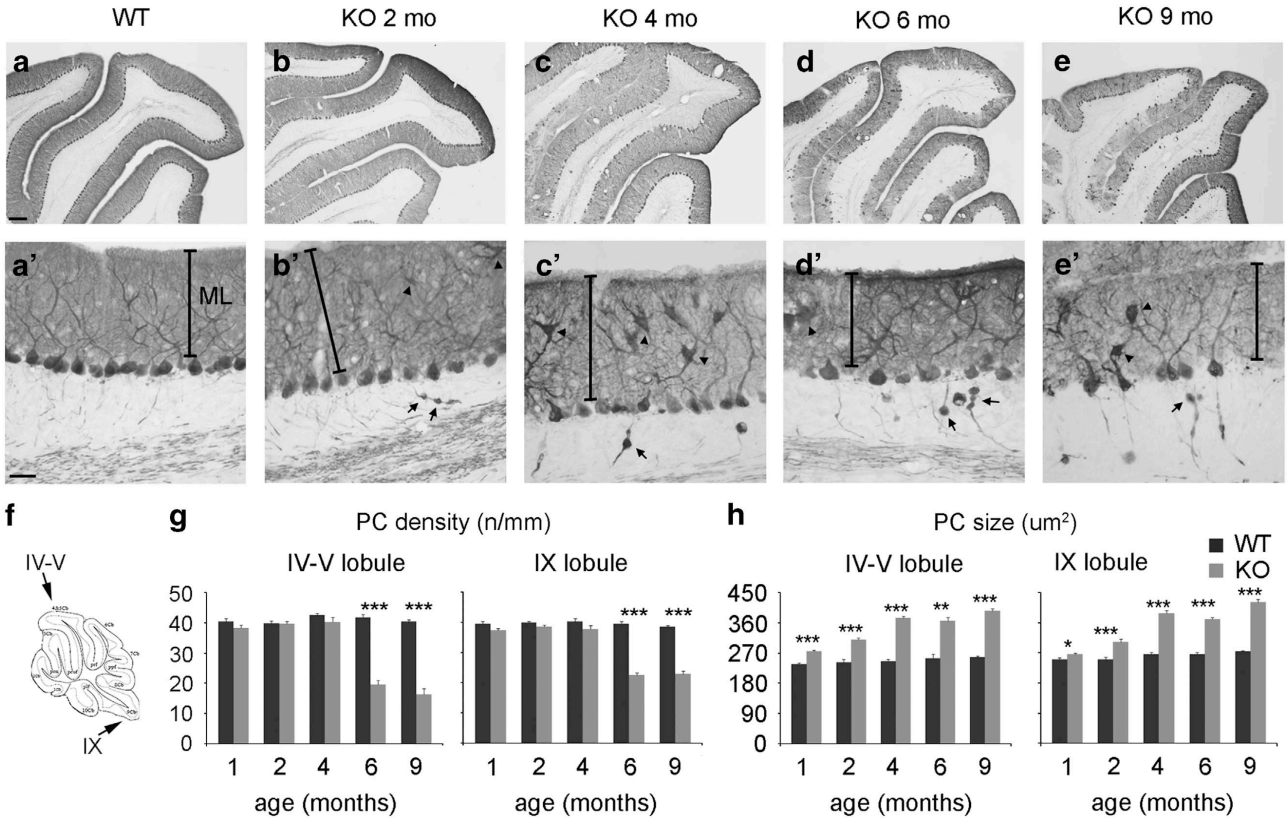
WT
KO 2 mo
KO 4 mo
KO 6 mo
KO 9 mo
a
b
c
d
e
a'
b'
c'
d'
e'
ML
f
IV-V
IX
g
PC density (n/mm)
IV-V lobule
IX lobule
50
40
30
20
10
0
1 2 4 6 9
age (months)
h
PC size (um²)
IV-V lobule
IX lobule
WT
KO
450
360
270
180
90
0
1 2 4 6 9
age (months)

Fig. 2

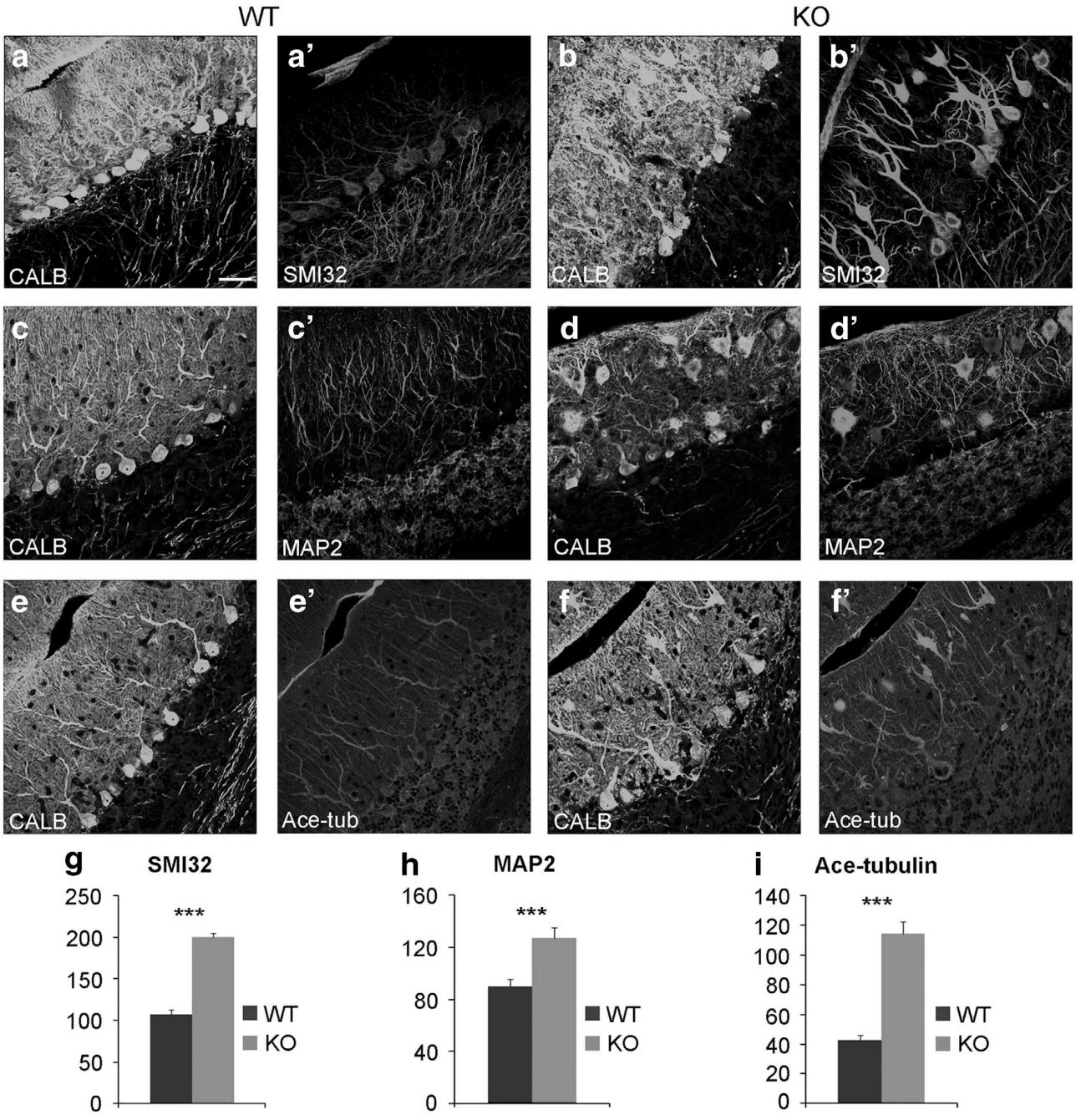
WT
KO
a
CALB
a'
SMI32
b
CALB
b'
SMI32
c
CALB
c'
MAP2
d
CALB
d'
MAP2
e
CALB
e'
Ace-tub
f
CALB
f'
Ace-tub
g
SMI32
250
200
150
100
50
0
***
WT
KO
h
MAP2
160
120
80
40
0
***
WT
KO
i
Ace-tubulin
140
120
100
80
60
40
20
0
***
WT
KO

Fig. 3

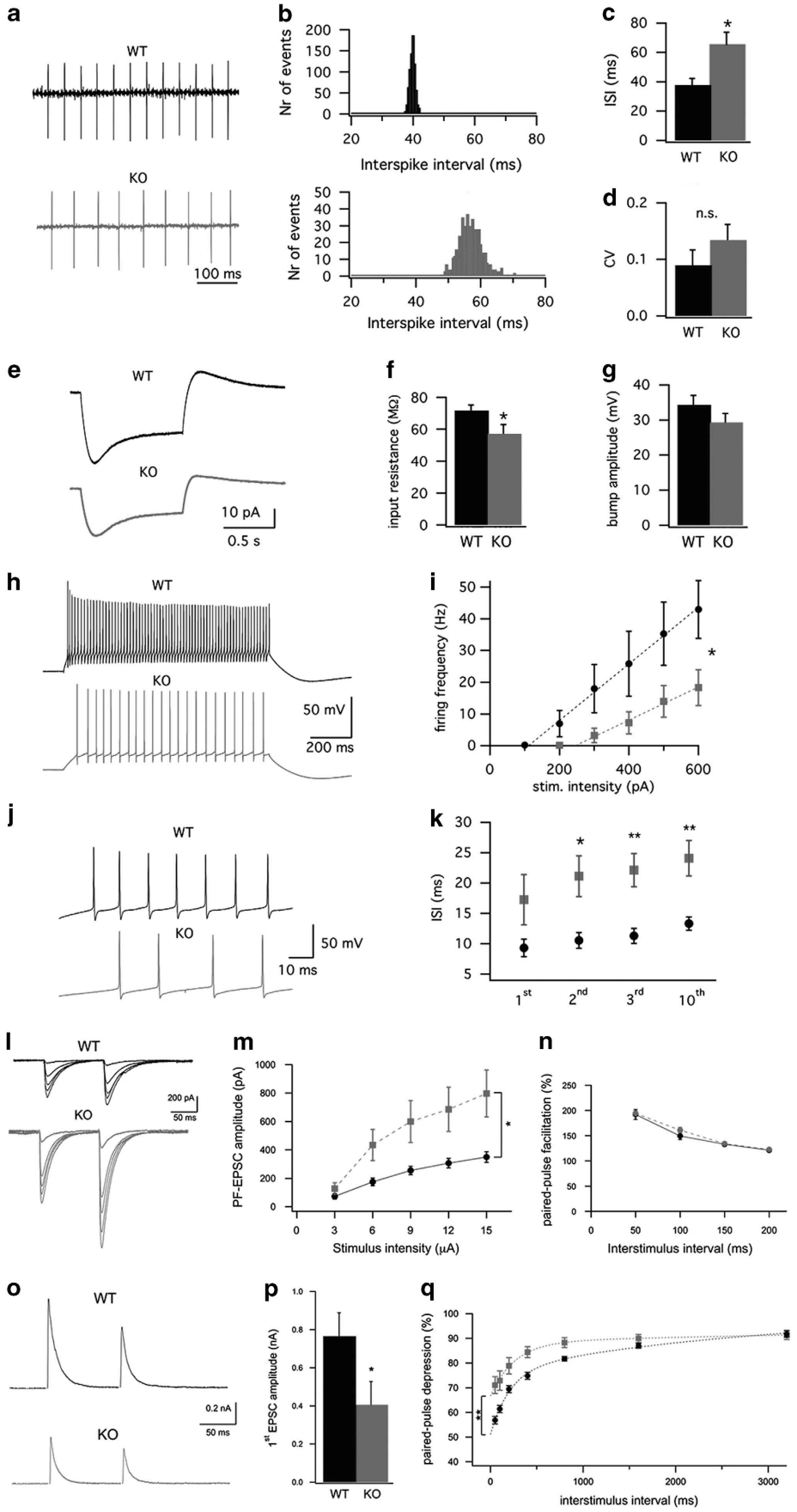
a
WT
KO
100 ms
b
Nr of events
Interspike interval (ms)
c
ISI (ms)
WT KO
d
CV
n.s.
WT KO
e
WT
KO
10 pA
0.5 s
f
input resistance (MΩ)
WT KO
g
bump amplitude (mV)
WT KO
h
WT
KO
50 mV
200 ms
i
firing frequency (Hz)
stim. intensity (pA)
j
WT
KO
50 mV
10 ms
k
ISI (ms)
1st 2nd 3rd 10th
l
WT
KO
200 pA
50 ms
m
PF-EPSC amplitude (pA)
Stimulus intensity (μA)
n
paired-pulse facilitation (%)
Interstimulus interval (ms)
o
WT
KO
0.2 nA
50 ms
p
1st EPSC amplitude (nA)
WT KO
q
paired-pulse depression (%)
interstimulus interval (ms)

Fig. 4

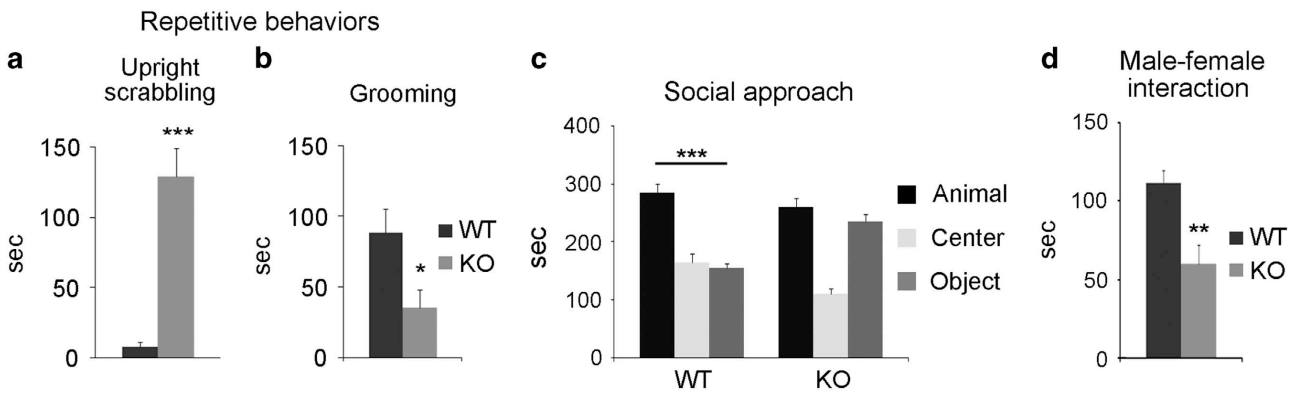
Repetitive behaviors
a
Upright scrabbling
***
150
100
50
0
sec
b
Grooming
150
100
50
0
sec
WT
KO
*
c
Social approach
400
300
200
100
0
sec
***
Animal
Center
Object
WT
KO
d
Male-female interaction
150
100
50
0
sec
**
WT
KO

Fig. 5